Reconfigurable Intelligent Surfaces Aided Energy Efficiency Maximization in Cell-Free Networks

Kewei Wang, Nan Qi, *Senior Member, IEEE*, Haoxuan Liu, Alexandros-Apostolos A. Boulogeorgos, *Senior Member, IEEE*, Theodoros A. Tsiftsis, *Senior Member, IEEE*, Ming Xiao, *Senior Member, IEEE*, Kai-Kit Wong *Fellow, IEEE*

***Abstract*—As we move towards next-generation wireless networks, the need for sustainability through energy efficiency (EE) concepts becomes more important than ever. Meanwhile, technology enablers, such as beamforming and reconfigurable intelligent surfaces (RISs), if appropriately used in a synergetic manner, can deliver profound excellence in terms of EE. Motivated by this, in this paper, we introduce an EE maximization policy that accounts for the rate demands of the end-users in RIS-assisted cell-free networks. The policy aims at performing joint optimization of the transmit beamforming vectors and the RIS phase-shift matrices in order to maximize the EE. In this direction, we first formulate the corresponding optimization problem, which is non-convex. To solve it, we rely on advanced optimization methods such as quadratic and Lagrangian dual transforms. Numerical results highlight the superiority of the presented policy in comparison to baseline approaches and reveal the most impactful network parameters.**

***Index Terms*—Reconfigurable intelligent surface, cell-free network, energy efficiency maximization, fractional programming, beamforming.**

I. Introduction

In beyond fifth generation and sixth generation networks, the emergence of vision centered on sustainable and green communication has sparked a crucial need for energy efficiency (EE) maxmization, which necessitates the development of innovative solutions [1] . Cell-free wireless networks [2] and reconfigurable intelligent surface (RIS) [3] are both revolutionary and complementary technologies, which are compatible and can improve EE of networks [4].

Kewei Wang, Nan Qi and Haoxuan Liu are with the Key Laboratory of Dynamic Cognitive System of Electromagnetic Spectrum Space, Nanjing University of Aeronautics and Astronautics, Nanjing 210016, China (e-mail: wangkw@nuaa.edu.cn, nanqi.commun@gmail.com, nuaalhx@nuaa.edu.cn). Kewei Wang and Nan Qi are also with the State Key Laboratory of Integrated Services Networks, Xidian University, Xi'an 710071, China.

Alexandros-Apostolos A. Boulogeorgos is with the Department Electrical and Computer Engineering, University of Western Macedonia, 50100 Kozani, Greece (aboulogeorgos@uowm.gr).

Theodoros A. Tsiftsis is with the Department of Informatics & Telecommunications, University of Thessaly, Lamia 35100, Greece (email: tsiftsis@uth.gr).

Ming Xiao is with the School of Electrical Engineering of KTH, Royal Institute of Technology, Stockholm, Sweden (e-mail: mingx@kth.se).

Kai-Kit Wong is with the Department of Electronic and Electrical Engineering, University College London, London WC1E 7JE, U.K. (e-mail: kai-kit.wong@ucl.ac.uk).

This work was supported in part by the National Natural Science Foundation of China (No. 62271253), Fundamental Research Funds for the Central Universities (No.NS2023018), and in part by the Open Research Fund of The State Key Laboratory of Integrated Services Networks, Xidian University under Grant ISN24-02.

For RIS-aided communications, considering power consumption, optimization in rate domain, such as weighed sum-rate maximization [5], fairness optimization [6], may not be a cost-effective choice, especially when communication resources are limited. As a result, in order to pursue sustainable communication, EE optimization is also an important issue. However, there is only a few works on EE maximization in RISs aided cell-free networks. In [7] and [8], the authors considered EE maximization in cell-based networks, in transmit beamforming state, the power allocation vectors instead of transmit beamforming vectors are optimized, which is not general enough for multi-antenna systems. In [9], the authors investigated EE maximization problem in RISs-aided cell-free networks, however, without considering rate threshold constraints of UEs and by using zero-force precoding, the transmit beamforming problem degraded into a power allocation problem, which limit performance.

Based on above observation, this letter contribute to the state-of-art of EE maximization in the following ways:

- We introduce an alternate optimization (AO) based EE maximization method in multi-RISs aided cell-free downlink scenario. Existing works, such as optimizing power allocation vector of BS [8], cell-based network [7], without rate threshold constraints [9], single RIS [7] are all the special cases of our general scenario, which require more mathematical transformations.
- By optimizing the transmit beamforming vectors and phase-shift matrices jointly, EE of the systems is maximized. In transmit beamforming, we transform the rate threshold constraints into second-cone constraints (SOC) and transform the sub-problem into convex form by nested usage of quadratic transform. In RIS phase-shift matrices subproblem, Lagrangian dual transform, quadratic transform, and semi-definite relaxation (SDR) are utilized.

II. System Model

A. Transmission Model

As shown in Fig. 1, a typical downlink scenario is considered, in which B base stations (BSs) serves K user equipments (UEs) equipped with single antenna cooperatively and simultaneously with the assistance of R distributed deployed RISs. The antenna number of each BS is N_t, and each RIS has the element number of N.

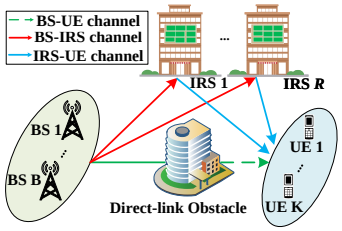

Fig. 1. Muti-RIS assisted cell-free network system.

We assume that perfect channel state information (CSI) is available[1], and the channel between BS b to RIS r, BS b to UE k, and RIS r to UE k is respectively denoted by $\mathbf{G}_{b,r} \in \mathbb{C}^{N\times N_t}$, $\mathbf{h}_{b,k}^H \in \mathbb{C}^{1\times N_t}$, and $\mathbf{v}_{r,k}^H \in \mathbb{C}^{1\times N}$. Due to the assumption that RISs can only change the phase of the incident signal, $\mathbf{\Phi}_r = \mathrm{diag}\left(\mathrm{e}^{j\theta_{r,1}}, \mathrm{e}^{j\theta_{r,2}}, \ldots, \mathrm{e}^{j\theta_{r,N}}\right) \in \mathbb{C}^{N\times N}$ can represent the phase-shift matrix for RIS r, where the phase-shift coefficient of n-th element in RIS r is denoted by $\mathrm{e}^{j\theta_{r,n}}$. After defining $\boldsymbol{\theta} = [\mathrm{vecdiag}\left(\mathbf{\Phi}_1\right)^T, \mathrm{vecdiag}\left(\mathbf{\Phi}_2\right)^T, \ldots, \mathrm{vecdiag}\left(\mathbf{\Phi}_R\right)^T]^T$, $\mathbf{G}_b = [\mathbf{G}_{b,1}^T, \ldots, \mathbf{G}_{b,R}^T]^T$, $\mathbf{V}_k = \mathrm{diag}([\mathbf{v}_{1,k}^T, \ldots, \mathbf{v}_{R,k}^T])$, the equivalent BS b-UE k channel can be formulated as[2]

$$\begin{aligned}\hat{\mathbf{h}}_{b,k}^H &= \mathbf{h}_{b,k}^H + \sum_{r=1}^{R} \mathbf{v}_{r,k}^H \mathbf{\Phi}_r^H \mathbf{G}_{b,r} \\ &= \mathbf{h}_{b,k}^H + \boldsymbol{\theta}^H \mathbf{V}_k^H \mathbf{G}_b.\end{aligned} \tag{1}$$

The received signal of UE k can be denoted by:

$$\begin{aligned}y_k &= \sum_{b=1}^{B}\sum_{j=1}^{K} \hat{\mathbf{h}}_{b,k}^H \mathbf{f}_{b,j} s_j + n_k \\ &= \sum_{b=1}^{B} \hat{\mathbf{h}}_{b,k}^H \mathbf{f}_{b,k} s_k + \sum_{j=1,j\neq k}^{K}\sum_{b=1}^{B} \hat{\mathbf{h}}_{b,k}^H \mathbf{f}_{b,j} s_j + n_k,\end{aligned} \tag{2}$$

where $\mathbf{f}_{b,k} \in \mathbb{C}^{N_t\times 1}$, $s_k \in \mathbb{C}^{1\times 1}$, and $n_k \sim \mathcal{CN}\left(0, \sigma_k^2\right)$ is the transmit beamforming vector of BS b for UE k, symbol sent to UE k from BSs with normalized power, and the additive white Gaussian noise (AWGN) at UE k with the noise power of σ_k^2. The signal-to-interference-plus-noise ratio (SINR) of UE k can be formulated as

$$\Gamma_k = \frac{\left|\sum_{b=1}^{B} \hat{\mathbf{h}}_{b,k}^H \mathbf{f}_{b,k}\right|^2}{\sum_{j=1,j\neq k}^{K}\left|\sum_{b=1}^{B} \hat{\mathbf{h}}_{b,k}^H \mathbf{f}_{b,j}\right|^2 + \sigma_k^2}. \tag{3}$$

The sum rate of UEs can be written as

$$\sum_{k=1}^{K} R_k = \sum_{k=1}^{K} \log_2\left(1+\Gamma_k\right). \tag{4}$$

B. Power Consumption Model

The total power consumption of the system includes four parts: i) beamforming power of BS, ii) static power of BS, iii) static power of UE, and iv) phase-shift power of RISs, which can be written as

$$P_c = \underbrace{\sum_{k=1}^{K} \mathrm{Tr}\left(\sum_{b=1}^{B} \mathbf{f}_{b,k}\mathbf{f}_{b,k}^H\right)}_{\text{beamforming power}} + \underbrace{\sum_{b=1}^{B} P_b^{BS} + \sum_{k=1}^{K} P_k^{UE} + P_c^{RIS}}_{\text{static power consumption of system}}, \tag{5}$$

where P_b^{BS}, P_k^{UE} and P_c^{RIS} is the static power consumption (circuit power) of BS b, UE k, and phase-shift power consumption of all RISs, respectively. The total phase-shift power consumption can be model as $P_c^{RIS} = RNP_e$, where P_e denote the power consumption of each element of RIS, which depends on the resolution of RIS phase shift[3].

C. Problem Formulation

In order to pursue sustainable and high cost-effective communication, we aim to maximize EE by optimizing the transmit beamforming vector of BSs and phase-shift matrices of RISs jointly, which can be written as

$$\max_{\mathbf{F},\boldsymbol{\theta}} \quad \frac{\sum_{k=1}^{K} R_k}{\sum_{k=1}^{K} \mathrm{Tr}\left(\sum_{b=1}^{B} \mathbf{f}_{b,k}\mathbf{f}_{b,k}^H\right) + P_{on}} \tag{6a}$$

$$\text{s.t.} \quad \sum_{k=1}^{K} \mathrm{Tr}\left(\mathbf{f}_{b,k}\mathbf{f}_{b,k}^H\right) \leqslant P_b, \forall b, \tag{6b}$$

$$r_{k,th} \leqslant R_k, \forall k, \tag{6c}$$

$$|\theta_n| = 1, \forall n, \tag{6d}$$

where $P_{on} = \sum_{b=1}^{B} P_b^{BS} + \sum_{k=1}^{K} P_k^{UE} + P_c^{RIS}$ represents the total static power consumption, $\mathbf{F}$, P_b, $r_{k,th}$, and θ_n denote the set of BS beamforming vectors, power budget of BS b, rate threshold of UE k, and the n-th entry of $\boldsymbol{\theta}$, respectively.

Note that through power budget constraints (6b) are convex, problem (6) is still non-convex due to variable coupled in fractional form of (6a), non-convex rate threshold constraints (6c), and non-convex unit-modulus constraints (6d) introduced by RIS, which is challenging to solve.

III. EE Maximization Algorithm Design

On account of variables coupled in (6a) and (6c), in this section, we present an AO based EE optimization algorithm. In each iteration, we first optimize $\mathbf{F}$ with fixed $\boldsymbol{\theta}$, then calculate $\boldsymbol{\theta}$ with given $\mathbf{F}$. Consequently, problem (6) can be divided into two sub-problems.

A. Transmit Beamforming Optimization

For transmit beamforming sub-problem, with a fixed $\boldsymbol{\theta}$, problem (6) can be written as

$$\max_{\mathbf{F}} \quad \frac{\sum_{k=1}^{K} R_k}{\sum_{k=1}^{K} \mathrm{Tr}\left(\sum_{b=1}^{B} \mathbf{f}_{b,k}\mathbf{f}_{b,k}^H\right) + P_{on}} \tag{7a}$$

$$\text{s.t.} \quad \sum_{k=1}^{K} \mathrm{Tr}\left(\mathbf{f}_{b,k}\mathbf{f}_{b,k}^H\right) \leqslant P_b, \forall b, \tag{7b}$$

$$r_{k,th} \leqslant R_k, \forall k. \tag{7c}$$

[1]Sensing devices can be deployed on nodes to endow them with ability for channel estimation, more information can be found in [1] and [5].

[2]Due to the substantial path loss in multi-hop channels, we disregarded the signals that were reflected between RISs on two or more times.

[3]For simplicity and without loss of generality, we assume that RISs have ideal analog phase-shift resolution for theoretical analysis. Note that solutions of different resolutions can be obtained through discretization.

Since (7a) is a complicated fraction, quadratic transform in [10] is applied, then (7) can be written as (8),

$$\max_{\mathbf{F},y} \ 2\mathrm{Re}\{y^H(\sum_{k=1}^{K} R_k)^{\frac{1}{2}}\} - |y|^2 (\sum_{k=1}^{K}\sum_{b=1}^{B} \|\mathbf{f}_{b,k}\|^2 + P_{on}) \quad (8a)$$

$$\text{s.t. } (7b), (7c), \quad (8b)$$

where auxiliary variable y has closed-form solution as

$$y^{opt} = \frac{\left(\sum_{k=1}^{K} R_k\right)^{\frac{1}{2}}}{\sum_{k=1}^{K} \mathrm{Tr}\left(\sum_{b=1}^{B} \mathbf{f}_{b,k}\mathbf{f}_{b,k}^H\right) + P_{on}}. \quad (9)$$

Since the second term of (8a) is convex, according to the convex and concave properties of composite functions [11], only when $\sum_{k=1}^{K} R_k$ is concave, the objective function of (8) is concave. However, R_k is also a fractional expression with respect to $\mathbf{F}$, which is difficult to handle.

Similarly, after applying quadratic transform again, the concavity can be proofed, and (8) can be reformulated as (10),

$$\max_{\mathbf{F},y,\{q_k\}} \ 2\mathrm{Re}\left\{y^H\left(\sum_{k=1}^{K}\log\left(1+\Gamma_k^{'}(\mathbf{F},\{q_k\})\right)\right)^{\frac{1}{2}}\right\} - |y|^2 (\sum_{k=1}^{K}\sum_{b=1}^{B} \|\mathbf{f}_{b,k}\|^2 + P_{on}) \quad (10a)$$

$$\text{s.t.} \quad (7b), \quad (10b)$$

$$\tau_k \leqslant \Gamma_k, \forall k, \quad (10c)$$

where $\Gamma_k^{'}(\mathbf{F},\{q_k\})$ can be written as (11), $q_k \in \mathbb{C}^{1\times 1}, \forall k$ is the auxiliary variable introduced by quadratic transform, τ_k is the corresponding SINR threshold, and $\tau_k = 2^{r_{k,th}} - 1, \forall k$,

$$\Gamma_k^{'}(\mathbf{F},\{q_k\}) = -|q_k|^2\left(\sum_{j=1,j\neq k}^{K}\left|\sum_{b=1}^{B}\hat{\mathbf{h}}_{b,k}^H\mathbf{f}_{b,j}\right|^2 + \sigma_k^2\right) + 2\mathrm{Re}\left\{q_k^H\left(\sum_{b=1}^{B}\hat{\mathbf{h}}_{b,k}^H\mathbf{f}_{b,k}\right)\right\}, \quad (11)$$

$$q_k^{opt} = \frac{\sum_{b=1}^{B}\hat{\mathbf{h}}_{b,k}^H\mathbf{f}_{b,k}}{\sum_{j=1,j\neq k}^{K}\left|\sum_{b=1}^{B}\hat{\mathbf{h}}_{b,k}^H\mathbf{f}_{b,j}\right|^2 + \sigma_k^2}, \forall k. \quad (12)$$

For constraints (7c), by defining $\mathbf{b}_k = \left[\mathbf{0}_{K\times 1}^H, \sigma_k^H\right]^H$, $\tilde{\mathbf{h}}_k^H = \left[\hat{\mathbf{h}}_{1,k}^H,\ldots,\hat{\mathbf{h}}_{B,k}^H\right], \tilde{\mathbf{f}}_k = \left[\mathbf{f}_{1,k}^H,\ldots,\mathbf{f}_{B,k}^H\right]^H, \tilde{\mathbf{f}} = \left[\tilde{\mathbf{f}}_1^H,\cdots,\tilde{\mathbf{f}}_K^H,0\right]^H, \mathbf{H}_k = \begin{bmatrix}\mathrm{blkdiag}(\tilde{\mathbf{h}}_k^H,\cdots,\tilde{\mathbf{h}}_k^H)\\ \mathbf{0}_{1\times BKN_t}\end{bmatrix}, \forall k$, it can be equivalently reformulated as (13), where $\mathrm{Im}(\cdot)$ is the operation of taking the imaginary part.

$$\left\|\mathbf{H}_k\tilde{\mathbf{f}} + \mathbf{b}_k\right\|_2 \leq \sqrt{1+\frac{1}{\tau_k}}\left(\sum_{b=1}^{B}\hat{\mathbf{h}}_{b,k}^H\mathbf{f}_{b,k}\right), \forall k, \quad (13a)$$

$$\mathrm{Im}\left\{\sum_{b=1}^{B}\hat{\mathbf{h}}_{b,k}^H\mathbf{f}_{b,k}\right\} = 0, \forall k. \quad (13b)$$

Therefore, (7) can be written as

$$\max_{\mathbf{F},y,\{q_k\}} \ (10a) \quad \text{s.t.} \quad (7b), (13), \quad (14)$$

which is actually a second-order cone program (SOCP) problem, and can be solved by CVX [12].

B. Phase-shift Matrices Optimization

For given $\mathbf{F}$, the phase-shift optimization sub-problem can be reduced into

$$\max_{\boldsymbol{\theta}} \ \sum_{k=1}^{K} R_k \quad (15a)$$

$$\text{s.t. } \tau_k \leqslant \Gamma_k, \forall k, \quad (15b)$$

$$|\theta_n| = 1, \forall n. \quad (15c)$$

Note that (15) is non-convex due to complicated fractional form in (15a), (15b), non-convex constraints (15b) and (15c).

Since (15b) is a fractional expression, similarly, by introducing auxiliary variable $\beta_k, \forall k$, (15b) can be written as

$$2\mathrm{Re}\{\beta_k^H(\sum_{b=1}^{B}\hat{\mathbf{h}}_{b,k}^H\mathbf{f}_{b,k})\} - |\beta_k|^2(\sum_{j\neq k}^{K}\left|\sum_{b=1}^{B}\hat{\mathbf{h}}_{b,k}^H\mathbf{f}_{b,j}\right|^2 + \sigma_k^2) \geq \tau_k, \quad (16)$$

where β_k have closed-form solution as

$$\beta_k^{opt} = \frac{\sum_{b=1}^{B}\hat{\mathbf{h}}_{b,k}^H\mathbf{f}_{b,k}}{\sum_{j=1,j\neq k}^{K}\left|\sum_{b=1}^{B}\hat{\mathbf{h}}_{b,k}^H\mathbf{f}_{b,j}\right|^2 + \sigma_k^2}, \forall k. \quad (17)$$

For non-convex unit-modulus constraints (15c), by defining $\bar{\boldsymbol{\theta}} = [\boldsymbol{\theta}^H 1]^H, \boldsymbol{\Theta} = \bar{\boldsymbol{\theta}}\bar{\boldsymbol{\theta}}^H$, (15c) can be written as

$$\mathrm{rank}\,(\boldsymbol{\Theta}) = 1, \quad (18a)$$

$$\boldsymbol{\Theta} \succeq 0. \quad (18b)$$

Correspondingly, by expanding $\hat{\mathbf{h}}_{b,k}^H$ according to (1), (16) can be written as

$$\mathrm{Tr}\,(\boldsymbol{\Psi}_k\boldsymbol{\Theta}) + c_k \leq 0, \forall k, \quad (19)$$

where $c_k, \forall k$ is constant unrelated to $\boldsymbol{\Theta}$,

$$\boldsymbol{\Psi}_k = \begin{bmatrix} |\beta_k|^2\sum_{j=1,j\neq k}^{K}\mathbf{q}_{k,j}\mathbf{q}_{k,j}^H & \mathbf{u}_k \\ \mathbf{u}_k^H & 0\end{bmatrix}, \forall k, \quad (20)$$

$$\mathbf{u}_k = |\beta_k|^2\sum_{j=1,j\neq k}^{K}\mathbf{q}_{k,j}\left(\sum_{b=1}^{B}\mathbf{f}_{b,j}^H\mathbf{h}_{b,k}\right) - \mathbf{q}_{k,k}\beta_k^H, \forall k, \quad (21)$$

$$\mathbf{q}_{k,j} = \sum_{b=1}^{B}\mathbf{V}_k^H\mathbf{G}_b\mathbf{f}_{b,j}, \forall k, j. \quad (22)$$

Therefore, (15) can be reformulated as

$$\max_{\boldsymbol{\Theta},\{\beta_k\}} \ (15a) \quad \text{s.t.} \quad (18), (19). \quad (23)$$

Note that in (23), the objective function (15a) is a complex non-convex form containing log function and fractions, which is difficult to deal with. In this paper, Lagrangian dual transform in [13] is utilized to take the fraction out of the logarithm function, and (15a) can be written as

$$\sum_{k=1}^{K}\log_2(1+\gamma_k) - \sum_{k=1}^{K}\gamma_k + \sum_{k=1}^{K}(1+\gamma_k)\frac{\left|\sum_{b=1}^{B}\hat{\mathbf{h}}_{b,k}^H\mathbf{f}_{b,k}\right|^2}{\sum_{j=1}^{K}\left|\sum_{b=1}^{B}\hat{\mathbf{h}}_{b,k}^H\mathbf{f}_{b,j}\right|^2 + \sigma_k^2}, \quad (24)$$

where $\gamma_k, \forall k$ is the auxiliary variable introduced by Lagrangian dual transform, which have closed-form solution by

$$\gamma_k^{opt} = \Gamma_k. \quad (25)$$

In (24), the third term includes fractional forms, the quadratic transform is applied once again, by introducing auxiliary variable $z_k, \forall k$, (15) can be reformulated as

$$\begin{aligned} \max_{\boldsymbol{\Theta},\{\beta_k\},\{\gamma_k\},\{z_k\}} \quad & \sum_{k=1}^{K} \log_2(1+\gamma_k) - \sum_{k=1}^{K} \gamma_k + \sum_{k=1}^{K} x_k(\boldsymbol{\theta},\{z_k\}) \\ \text{s.t.} \quad & (18),(19), \end{aligned} \tag{26}$$

where $x_k(\boldsymbol{\theta},\{z_k\})$ is a function of $\boldsymbol{\theta}$ and $\{z_k\}$, and

$$\begin{aligned} x_k =& 2\left(1+\gamma_k\right) \mathrm{Re}\left\{ z_k^H \left(\sum_{b=1}^{B} \hat{\mathbf{h}}_{b,k}^H \mathbf{f}_{b,k} \right) \right\} \\ & - \left(1+\gamma_k\right) |z_k|^2 \left(\sum_{j=1}^{K} \left| \sum_{b=1}^{B} \hat{\mathbf{h}}_{b,k}^H \mathbf{f}_{b,j} \right|^2 + \sigma_k^2 \right), \forall k, \end{aligned} \tag{27}$$

$$z_k^{opt} = \frac{\sum_{b=1}^{B} \hat{\mathbf{h}}_{b,k}^H \mathbf{f}_{b,k}}{\sum_{j=1}^{K} \left| \sum_{b=1}^{B} \hat{\mathbf{h}}_{b,k}^H \mathbf{f}_{b,j} \right|^2 + \sigma_k^2}. \tag{28}$$

Note that the objective function of (26) is a concave quadratic function, and can be written as $\boldsymbol{\theta}^H \mathbf{M} \boldsymbol{\theta} + 2\mathrm{Re}\left\{\boldsymbol{\theta}^H \mathbf{n}\right\} + d$, where d is a constant unrelated to $\boldsymbol{\theta}$, and

$$\mathbf{M} = -\sum_{k=1}^{K} (1+\gamma_k) |z_k|^2 \sum_{j=1}^{K} \left(\mathbf{q}_{k,j} \mathbf{q}_{k,j}^H \right), \tag{29}$$

$$\mathbf{n} = \sum_{k=1}^{K} (1+\gamma_k) \left[z_k^H \mathbf{q}_{k,j} - |z_k|^2 \sum_{j=1}^{K} \left(\mathbf{q}_{k,j} \sum_{b=1}^{B} \mathbf{f}_{b,j}^H \mathbf{h}_{b,k} \right) \right]. \tag{30}$$

Consequently, by defining $\boldsymbol{\Lambda} = \begin{bmatrix} \mathbf{M} & \mathbf{n} \\ \mathbf{n}^H & 0 \end{bmatrix}$, (15) and (23) can be reformulated as

$$\begin{aligned} \max_{\boldsymbol{\Theta},\{\beta_k\},\{\gamma_k\},\{z_k\}} \quad & \mathrm{Tr}\left(\boldsymbol{\Theta}\boldsymbol{\Lambda}\right) + d \\ \text{s.t.} \quad & (18),(19), \end{aligned} \tag{31}$$

where $\beta_k, \gamma_k, z_k, \forall k$ are given in closed form according to (17), (25), and (28), respectively.

Note that, (31) can be viewed as a nearly convex semi-definite program (SDP) problem, with the exception of non-convex rank-1 constraint (18a). In this paper, we utilize the widely used SDR method. Specially, we first relax constraint (18a) to solve SDP problem, then recover high-quality rank-1 solution by Gaussian randomization [6], which is omitted due to space limitation.

Therefore, the presented EE maximization algorithm is summarized in **Algorithm 1**. Since the transmit beamforming sub-problem and RIS phase-shift sub-problem are blocks of alternating optimization or block coordinate descent, we can ensure that the objective function monotonically increases, thus the convergence can be guaranteed. And the presented algorithm costs the complexity of $\mathcal{O}\left(I_1\left(\log_2(1/\epsilon)\cdot\left((NR+1)^{4.5}+BK(N_t)^{3.5}\right)\right)\right)$, where I_1 is the number of iterations, and ϵ denotes the target precision [6].

Algorithm 1 Proposed EE maximization algorithm for (6)

1: **Initialize** $\mathbf{f}_{b,k}, \mathbf{v}_{r,k}^H, \mathbf{h}_{b,k}^H, \mathbf{G}_{b,r}^H, \forall b,r,k, \boldsymbol{\theta}$, and the random sampling number for SDR $\mu, \mu > 0$;
2: **Update** equivalent channel $\mathbf{h}_{b,k}^H, \forall b,k$ according to (1);
3: **Repeat**
4: **Update** y and $q_k, \forall k$ according to (9) and (12);
5: **Update** $\mathbf{F}$ by solving SOCP problem (14);
6: **Update** $\beta_k, \gamma_k, z_k, \forall k$ according to (17), (25), and (28), respectively;
7: **Update** $\boldsymbol{\Theta}'$ by solving relaxed SDP problem;
8: **For** $i = 1:\mu$
9: **Update** $\boldsymbol{\Theta}_i$ from $\boldsymbol{\Theta}'$ through SDR;
10: **End for**
11: **Update** $\boldsymbol{\Theta}$ by selecting the best from $\{\Theta_i\}$;
12: **Update** $\boldsymbol{\theta}$ from $\boldsymbol{\Theta}$;
13: **Update** equivalent channel $\mathbf{h}_{b,k}^H, \forall b,k$ according to (1);
14: **Until** termination criterion is met.

IV. Numerical Results

In this section, numerical results are provided to verify the effectiveness of the presented EE optimization algorithm. As shown in Fig. 2, we assume that $B = 2, R = 2, K = 4$, BSs located at $(0\text{m}, 280\text{m})$, and $(560\text{m}, 280\text{m})$, RISs located at $(100\text{m}, 100\text{m})$, and $(250\text{m}, 50\text{m})$, and UEs follow Poisson distribution.

For the channel model, since direct-link obstacle exist between BSs and UEs, we assume that BSs-UEs channel follow Rayleigh fading, BSs-RISs and RISs-UEs channel follow Rician fading. We utilize the same large-scale and small-scale channel model as [6], and set path loss of reference distance of 1m to be $\rho = -30$dB, the path-loss exponent of line-of-sight (LoS) and non-LoS link, and the Rician factor is set to be $\varepsilon_{LoS} = 2.2$, $\varepsilon_{nLoS} = 3.75$, and 3, respectively. For the power consumption, we assume that $P_b^{BS} = 10\text{dBW}, P_k^{UE} = 10\text{dBm}, \forall b,k$, and the phase-shift power consumption of each element P_e for 1-bit, 2-bit, 3-bit, and analog phase shift is set to be 5dBm, 10dBm, 15dBm, and 25dBm, respectively. In the following figure, we default the phase-shift mode to analog unless otherwise specified.

Fig. 3 shows the convergence behaviour of several algorithms, and parameters are initialized to the same value. In each iteration, one transmit beamforming or phase-shift matrices optimizing sub-problem are solved. Compared with baseline algorithms, the proposed algorithm converges fast.

Fig. 4 illustrates the performance comparison of relevant methods, and all the curves are averaged over 100 channel realization. EE of this algorithm outperforms several different baseline algorithms. As power budget increases, EE of this algorithm first increases and then remains almost unchanged, implying that when power budget reaches a certain threshold, simply increasing it may not be beneficial to improving EE. On the contrary, when power budget is large enough, with it increasing, EE of maximum ratio transmission (MRT)-based and fairness-based algorithms will decrease, since the denominator of objective function will also boost with the power budget. Moreover, algorithms with random RIS phase-shift even have worse EE performance than those without RISs, this is because introducing RIS (even with random phase-shift) will cause more power, which explained the importance of optimizing phase-shift matrices of RISs in improving system EE.

Fig. 5 presents how average EE and sum-rate (SR) vary with

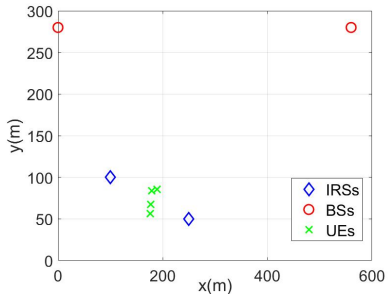

Fig. 2. Simulation scenario setup

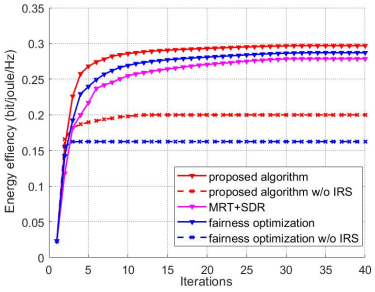

Fig. 3. Convergence performance of algorithms when $N = 25, N_t = 4, r_k = 0, \forall k, P_b = 30\text{dBm}, \forall b$

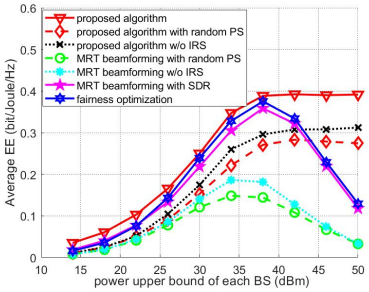

Fig. 4. EE performance comparison of different methods when $N = 16, N_t = 4, r_{k,th} = 0, \forall k$

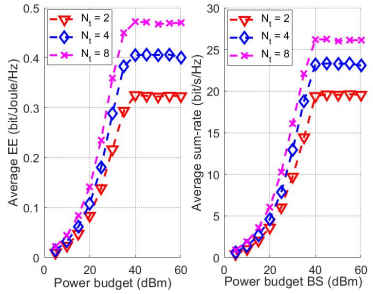

Fig. 5. Averge EE and SR vs N_t and P_b when $N = 36, P_b = 30\text{dBm}, \forall b, r_{k,th} = 0, \forall k$

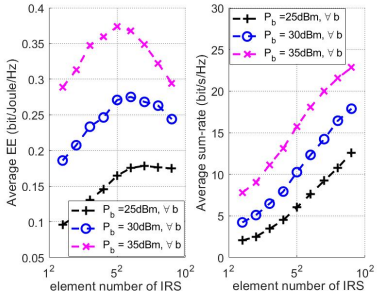

Fig. 6. Averge EE and SR vs N and P_b when $N_t = 4, r_{k,th} = 0, \forall k$

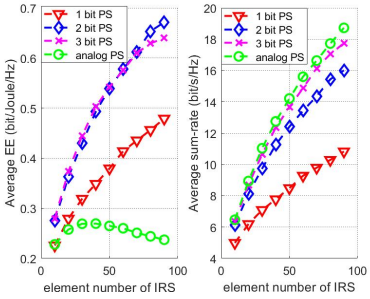

Fig. 7. Averge EE and SR vs phase-shift mode of RISs when $N_t = 4, r_{k,th} = 0, \forall k, r_{k,th} = 0, \forall k, P_b = 30\text{dBm}, \forall b$

power budget and antenna number of BSs, and all the curves are averaged over 100 channel realization. When the power budget reaches a certain limit, further improvement could not result in better EE performance, which is consistent with the conclusion in Fig. 4. Moreover, though increasing N_t can improve both EE and SR, it will cause heavier hardware costs.

In Fig. 6, the impact of element number of RISs and power budget on average EE and SR are analyzed, and all the curves are averaged over 100 channel realization. Through introducing more element number can bring SR improvement, it may reduce system EE since elements will cost power.

Fig. 7 demonstrates how average EE and SR vary with the phase-shift mode of RISs, and all the curves are averaged over 100 channel realization. Through more accurate resolution of phase shift will bring higher SR, considering the power consumption of elements, 2-bit and 3-bit phase-shift mode can acquire better EE performance.

V. Conclusion

This paper presented an AO based EE maximization method in multi-RIS aided cell-free downlink scenario, by jointly optimizing the transmit beamforming vectors and phase-shift matrices, EE of the systems is maximized. Finally, we analyzed the impact of different parameters on the simulation results, such as element number of RIS, power budget, etc.

References

[1] Q. Wu, S. Zhang, B. Zheng, C. You, and R. Zhang, "Intelligent reflecting surface-aided wireless communications: A tutorial," *IEEE Trans. Commun.*, vol. 69, no. 5, pp. 3313–3351, May 2021.

[2] H. Q. Ngo, A. Ashikhmin, H. Yang, E. G. Larsson, and T. L. Marzetta, "Cell-free massive MIMO versus small cells," *IEEE Trans. Wirel. Commun.*, vol. 16, no. 3, pp. 1834–1850, Mar 2017.

[3] Q. Wu and R. Zhang, "Towards smart and reconfigurable environment: Intelligent reflecting surface aided wireless network," *IEEE Commun. Mag.*, vol. 58, no. 1, pp. 106–112, Jan 2020.

[4] J. Tang, Z. Peng, D. K. C. So, X. Zhang, K.-K. Wong, and J. A. Chambers, "Energy efficiency optimization for a multiuser IRS-aided MISO system with SWIPT," *IEEE Trans. Commun.*, vol. 71, no. 10, pp. 5950–5962, Jul 2023.

[5] K. Wang, N. Qi, X. Guan, Q. Shi, M. Xiao, S. Jin, and K.-K. Wong, "Transmit/passive beamforming design for multi-IRS assisted cell-free MIMO networks," *IEEE Syst. J.*, vol. 17, no. 4, pp. 6282–6291, Oct 2023.

[6] K. Wang, N. Qi, M. Xiao, S. Hu, and B. Sihlbom, "Fairness-aware location and hybrid beamforming optimization in IRSs-aided cell-free MIMO system," in *IEEE/CIC International Conference on Communications in China (ICCC)*, 2023, pp. 1–6.

[7] C. Huang, A. Zappone, G. C. Alexandropoulos, M. Debbah, and C. Yuen, "Reconfigurable intelligent surfaces for energy efficiency in wireless communication," *IEEE Trans. Wirel. Commun.*, vol. 18, no. 8, pp. 4157–4170, Jun 2019.

[8] S. Jia, X. Yuan, and Y.-C. Liang, "Reconfigurable intelligent surfaces for energy efficiency in D2D communication network," *IEEE Wirel. Commun. Lett.*, vol. 10, no. 3, pp. 683–687, Dec 2021.

[9] Y. Zhang, B. Di, H. Zhang, J. Lin, C. Xu, D. Zhang, Y. Li, and L. Song, "Beyond cell-free MIMO: Energy efficient reconfigurable intelligent surface aided cell-free MIMO communications," *IEEE Trans. Cogn. Commun. Netw.*, vol. 7, no. 2, pp. 412–426, Jun 2021.

[10] K. Shen and W. Yu, "Fractional programming for communication systems-part I: Power control and beamforming," *IEEE Trans. Signal Process.*, vol. 66, no. 10, pp. 2616–2630, May 15 2018.

[11] S. Boyd, S. P. Boyd, and L. Vandenberghe, *Convex optimization*. Cambridge university press, 2004.

[12] M. Grant and S. Boyd, "CVX: Matlab software for disciplined convex programming, version 2.1," 2014.

[13] K. Shen and W. Yu, "Fractional programming for communication systems-part II: Uplink scheduling via matching," *IEEE Trans. Signal Process.*, vol. 66, no. 10, pp. 2631–2644, May 15 2018.